Published in final edited form as:
Bone. 2010 April ; 46(4): 1188–1196. doi:10.1016/j.bone.2009.12.002.

THE CYSTIC FIBROSIS TRANSMEMBRANE CONDUCTANCE REGULATOR (CFTR) IS EXPRESSED IN MATURATION STAGE AMELOBLASTS, ODONTOBLASTS AND BONE CELLS

Antonius Bronckers[1,*], **Lida Kalogeraki**[1,2], **Huub J.N. Jorna**[3], **Martina Wilke**[3], **Theodore J. Bervoets**[1], **Donacian M. Lyaruu**[1], **Behrouz Zandieh-Doulabi**[1,4], **Pamela DenBesten**[5], and **Hugo de Jonge**[3]

[1] Department of Oral Cell Biology, Academic Centre for Dentistry Amsterdam (ACTA), Research Institute MOVE, University of Amsterdam and VU University Amsterdam, The Netherlands [2] Department of Periodontology Academic Centre for Dentistry Amsterdam (ACTA), University of Amsterdam and VU University Amsterdam, The Netherlands [3] Department of Biochemistry, Erasmus University Medical Center, Rotterdam, The Netherlands [4] Department of Orthopedics, Research Institute MOVE VU-University Medical Center Amsterdam [5] Department of Orofacial Sciences, University of California, San Francisco, Box 0422, 707 Parnassus Ave, San Francisco, CA, USA

Abstract

Patients with cystic fibrosis (CF) have mild defects in dental enamel. The gene mutated in these patients is *CFTR*, a Cl^- channel involved in transepithelial salt- and water transport and bicarbonate secretion. We tested the hypothesis that Cftr channels are present and operating in the plasma membranes of mouse ameloblasts.

Tissue sections of young mouse jaws and fetal human jaws were immunostained with various anti-Cftr antibodies. Specificity of the antibodies was validated in *Cftr*-deficient murine and human tissues. Immunostaining for Cftr was obtained in the apical plasma membranes of mouse maturation ameloblasts of both incisor and molar tooth germs. A granular intracellular immunostaining of variable intensity was also noted in bone cells and odontoblasts. In *Cftr*-deficient mice the incisors were chalky white and eroded much faster than in wild type mice. Histologically, only maturation ameloblasts of incisors were structurally affected in *Cftr*-deficient mice. Some antibody species gave also a positive cytosolic staining in *Cftr*-deficient cells. Transcripts of *Cftr* were found in maturation ameloblasts, odontoblasts and bone cells. Similar data were obtained in forming human dentin and bone.

We conclude that Cftr protein locates in the apical plasma membranes of mouse maturation ameloblasts. In mouse incisors *Cftr* is critical for completion of enamel mineralization and conceivably functions as a regulator of pH during rapid crystal growth. Osteopenia found in CF patients as well as in *Cftr*-deficient mice is likely associated with defective *Cftr* operating in bone cells.

Corresponding author: ALJJ Bronckers, Oral Cell Biology ACTA, Vrije Universiteit, Van der Boechorststr 7, 1081 BT Amsterdam, The Netherlands, Tel: +31-20-4448665, Fax: +31-20-4448683, A.Bronckers@vumc.nl.

Keywords

CFTR; immunostaining; ameloblasts; osteoblasts; osteoclasts; Cftr-knockout

Introduction

Cystic fibrosis (CF) is the most common lethal autosomal recessive disease in Caucasians, caused by mutations in the cystic fibrosis transmembrane conductance regulator (*CFTR*) gene [1]. CFTR is a chloride channel that is regulated by cyclic AMP-dependent protein phosphorylation and is required for transepithelial salt and water transport. The CFTR protein consists of two homologous repeats, each containing six membrane-spanning domains (MSD1&2, Fig. 1) followed by an intracellular nucleotide-binding domain (NBD1&NBD2). These two half-molecules are joined by an intracellular regulatory or R-domain. The MSD-domains form the central pore through which Cl^- ions cross the cell membrane. Recent evidence revealed that CFTR is also crucial for bicarbonate secretion [2–4]. Apart from its secretory function, CFTR controls the activity of other channels and transporters including the Na^+/H^+ exchanger (NHE), HCO_3^-/Cl^- exchanger and cotransporters, intermediate conductance outwardly *r*ectifying (ICOR) Cl^- channels, and Ca^{+2}- and volume-activated Cl^- channels (for review see [5,6]).

The tissues affected in CF patients include sweat glands, intestine, bile duct, pancreatic ducts, respiratory epithelia, submandibular glands, uterus and vas deferens [7–13]. Dental enamel, a product of epithelial cells is also (mildly) affected in some CF patients [14–17].

It was unclear for a long time whether enamel defects in CF patients were direct effects due to dysfunctional ameloblasts or secondary effects that follow medication, respiratory problems or malnutrition caused by intestinal obstruction, pancreatic insufficiency or poor intestinal absorption [14–17]. Enamel defects seen in *Cftr* knockout mice [18,19], and detection of *Cftr* mRNA transcripts in developing teeth of wild type mice [20] suggested that this chloride channel operates also in ameloblasts.

The high rate of mineral acquisition during advanced stage enamel formation generates large quantities of protons and it has been proposed that ameloblasts buffer these protons by secreting bicarbonates into the enamel space [21–24]. Buffering these protons to near neutrality would enable further mineral growth [21,23]. What molecular mechanisms are responsible for such vectorial bicarbonate secretion and at which developmental stage this happens is unknown. Ameloblasts form enamel in two steps: in secretory stage they secrete an enamel matrix that initiates and fosters formation of thin enamel crystals [reviewed by [21,22]). This is followed by maturation stage. During first half of maturation stage the matrix is degraded and removed along with moderate increase in mineral. The second half of maturation stage when mineral acquisition is very high the (calculated) proton production is substantial [24]. In maturation phase two morphologically different types of cells have been recognized: ruffle-ended ameloblasts (the majority of the cells, with well developed membrane invaginations at their apical membranes), and smooth-ended ameloblasts with a smooth apical membrane [25]. During enamel maturation groups of these cells cyclically transform from ruffle-ended into smooth-ended cells and back multiple times, a process called modulation. Modulation is associated with alternation between narrow bands of enamel with neutral pH and much wider bands with slightly acidic pH, corresponding with smooth-ended cells and ruffle-ended cells, respectively [26–28]. The acidification is presumably is due to crystal growth. However in *Cftr* −/− mice maturation stage enamel is acidic, neutral pH bands are lacking [23] and matrix is retained [18]. The mutant ameloblasts do not modulate as assessed by failure to stain with glyoxal bis (2-hydroxyanil) (GHBA) [23] and enamel mineral accretion is severely reduced

[17,18,19,29]. These data suggest that a *Cftr* is critical for ameloblast modulation, pH regulation and for completion of enamel mineralization. Transcipts for *Cftr* mRNA have been detected in apical parts of mouse incisors and molars tooth germs [20]. The cells that express *Cftr* however have not been identified.

Given the relevance of *Cftr* for formation of fully matured enamel we tested the hypothesis that *Cftr* is expressed in the apical plasma membrane of maturation ameloblasts where it serves a critical role in pH regulation in developing enamel.

Materials and methods

Tissues

Jaws were collected from *Cftr* null mice (congenic FVB, three pups aged 13–17 days; five adult mice, aged 100–172 days), and littermate wild type controls (three pups and three adults). These ages covered all stages of enamel development in molar tooth germs and incisors. In addition, jaws from hamster (*Mesocricetus auratus L*) pups (total of 3, aged 3–7 days) and 16–20 week human fetal jaws (archival tissues) were used. Mice with targeted disruption in the *Cftr* gene ($Cftr^{tm2Cam}$ knockout mice, backcrossed for more than 12 generations into the FVB background; Cftr −/−) were originally obtained from Dr. William Colledge (Cambridge, UK) [30]. The *Cftr* gene codes for a 1480 amino acid glycoprotein with molecular mass of 170 kD. The insertion of a HPRT minigene into the coding sequence of the murine cystic fibrosis gene (*Cftr*) at arg 487 introduced a termination codon in frame with the *Cftr* coding sequence to terminate prematurely the cftr protein within the first nucleotide binding domain (NBD1, Fig 1). The remaining portion consists of the N-terminal part and the first membrane-spanning domain (MSD1); this truncated Cftr-fragment is very labile and insoluble, and is degraded via proteasomes immediately after synthesis. The *Cftr*−/− mouse strain was kept on solid food in the animal facility at the Erasmus Medical Center in Rotterdam (The Netherlands) and genotyped using DNA from tail clippings. To reduce the incidence of intestinal obstruction, polyethylene glycol (17.6 mM; Klean Prep) was added to the drinking water. Human primary osteoblasts were obtained by outgrowth of cells from human morselized bone chips grown as cultures and provided by the Department of Orthopedics of the VU-University Hospital in Amsterdam. Freshly extracted human wisdom teeth were obtained from the Department of Oral and Maxillofacial Surgery of Academic Centre for Dentistry Amsterdam (ACTA). All animal procedures were approved by the Committee for Animal Care using national standards for treatment of animals. Collection of human material was approved by Medical Ethical Committees, and with informed consent of the patients.

Histological procedures

Mandibles and maxillae were excised, freed from skin and fixed by immersion in 5% paraformaldehyde in 0.1 M phosphate buffer and 2% sucrose (pH 7.3) overnight and rinsed in phosphate buffer. Some samples were decalcified in 5% EDTA containing 0.8 % formalin at 4°C for 3 weeks. Decalcified and non-decalcified tissues were embedded in paraffin wax and serial sections were made in a sagittal or cross-sectional plane 5–7 micrometer thick and mounted on polylysin-coated glass slides. Immediately before immunostaining sections were dewaxed in three changes of xylene and rehydrated using descending concentrations of ethanol. For orientation and selection of appropriate stages of differentation every tenth section was routinely stained with hematoxylin-eosin (HE). To compare staining of the different antibodies series of three adjacent sections from the same block were chosen and stained with each of the antibodies.

Antibodies

Four different Cftr antibodies were used, two raised against peptide sequences from human CFTR and two against sequences from mouse Cftr, all located in the part of the *Cftr* gene that had been truncated in the *Cftr*-null mutant mice (Fig. 1). A mouse monoclonal antibody to human CFTR-C-terminus (clone 24–1) was purchased from R&D Systems Europe, Abingdon, UK (catalogue MAB25031). According to specifications of the manufacturer clone 24–1 was raised against human *CFTR* exon 23 and 24 (amino acids 1377-1480) conjugated to gluthathion-S-transferase. The rabbit polyclonal anti-mouse Cftr antibody MD1314 is a new version of antibody R3195 [31,32] and was raised against the 13-amino acid COOH terminal peptide sequence of rodent Cftr (amino acids 1468-1480), conjugated to bovine thyroglobulin. The antibodies were affinity purified on a peptide-epoxide activated Sepharose column, eluted with 4.9 mol/L $MgCl_2$, dialyzed and concentrated. Rat monoclonal 3G11, raised against the purified first nucleotide binding domain (NBD1) of mouse Cftr [33], was a kind gift of Prof. William E. Balch, Dept of Cell Biology, The Scripps Research Institute, La Jolla, CA 92037, USA. To specifically detect CFTR in human tissues rabbit antibody CC24 was raised against peptide sequence 693-716 of the human CFTR molecule and affinity purified (Fig. 1; [34, 35].

Immunostaining

Dewaxed and rehydrated paraffin sections were washed in phosphate saline buffer (PBS). After blocking endogenous peroxidase by incubation for 3 min in 3% hydrogen peroxide in PBS, antigen retrieval was performed by heating sections in 10 mM of citrate buffer pH 6.0 in a microwave for 20 min at 95°C. When mouse monoclonal antibodies (clone 24-1) were used to stain mouse tissues, endogenous mouse immunoglobulines were blocked with several rounds of blocking solutions from a Histomouse kit (Zymed/Invitrogen, CA, USA) prior to incubation with primary antibodies. All antibody species were stained with anti-mouse, anti-rabbit and anti-rat ABC-peroxidase Vectastain kits (Elite, Vector, Burlingame, CA, USA). Sections were incubated with the first antibodies overnight at 4°C. Dilutions of the primary antibodies were 1:100–1:200 for clone 24-1 (1–2 μg/ml final concentrations); 1:200 for MD1314 (final concentration 1 μg/ml), 1:50 to 1:100 for 3G11 (final concentration 10–20 μg/ml) and 1:100 for CC24 (final concentration 1.2 μg/ml). As (negative) controls primary antibodies were replaced by non-immune IgG from rat, mouse or rabbit in the same concentrations (Dakocytomation, Glostrup, Denmark). After washing in PBS biotinylated secondary antibodies were applied for 1 h at room temperature. Subsequently the sections were washed and incubated with the Avidin-Biotin peroxidase Complex for 1 hour. The immunostaining was developed with diamino benzidin (DAB kit, Vector) and counterstained with methyl green or hematoxylin.

Validation of specificity of antibodies

MD1314, 24-1 and 3G11 were tested on incisors from *Cftr*-deficient mice to investigate whether the immunostaining was negative. Sections were selected containing early stages of ameloblast maturation before the mutation caused severe histological changes in the ameloblast structure. To validate the CC24 anti-human CFTR antibody rectal biopsies obtained from healthy adult patients (positive controls) and from homozygous ΔF508 CF patients (functional knockout, negative controls) were used.

Real Time Reversed Transcription Polymerase Chain Reaction (RT-PCR)

Prior to RNA isolation, all tissue samples were processed with MagNALyser (Roche Diagnostics, Almere, The Netherlands) according to the manufacturer's instructions. Total RNA was extracted by the Trizol extraction method (Invitrogen) from freshly isolated mouse kidney, mouse tongue and rat maturation ameloblasts (collected by microdissection from adult

rat mandibular incisors according [28]). Total RNA from human dental pulp was isolated using the MagNA Pure LC isolation robot and a tissue RNA isolation kit (Roche Diagnostics). Total RNA from mouse calvarial osteoblast-like cell line MC3T3 and primary human osteoblasts (3rd passage) from hip bone was obtained using the NucleoSpin RNA/protein kit (Macherey-Nagel, Düren, Germany) according to the manufacturers' instructions. First strand cDNA synthesis was performed in a 25 μl reverse transcription reaction buffer containing 100 ng of total RNA; 1 × Transcriptor RT buffer; 1 mM of each dNTP; 0.08 U random primers; 10 U protector RNAse inhibitor and 5 U reverse transcriptase (Roche Diagnostics). The reactions were incubated at 42°C for 45 min, followed by 95°C for 5 min to inactivate the transcriptase. For each PCR reaction 10-fold diluted cDNA from mouse MC3T3, kidney (positive control) and tongue (negative control), rat ameloblasts and human Universal Reference RNA (Clontech Mountain View CA, USA; cat. No 636538) were used. Universal reference RNA is a pool of total human RNA from a collection of different tissues, a positive control for human CFTR). Real-time PCR analysis was performed using the LightCycler 480 system based on SYBR Green I dye (Roche Applied Science, Indianapolis, IN, USA). cDNA was amplified according to the following parameters: a 10 min activation of hot start enzyme at 95°C followed by 50 cycles of a two step amplification program consisting of 10 sec denaturation at 95°C and 30 sec annealing, elongation and extension at 63°C. For human *CFTR* the following primers were used: forward primer starting in exon 4: 5′caaggaggaacgctctatcg-3 and reverse primer: 5′ gtgccaatgcaagtccttca-3′ (ending in exon 6, nucleotides 471-727; expected length 257 bp, GI: NM_000492). For mouse *Cftr* forward primers starting in exon 4: 5′gccatttaccttggcataggc-3′ and reverse primer: 5′gccaaggcaagtccttcatca-3′ (ending in exon 5; nucleotides 435-669, expected length 235, GI: NM_021050.2). Independent PCR fragments, derived from the amplified CFTR/Cftr fragments, were sequenced using the BigDye Terminator Cycle Sequencing V3.1 Ready Reaction kit (Applied Biosystems, Nieuwerkerk aan de Ijssel, The Netherlands) and analyzed on an ABI PRISM 3100 Genetic Analyzer.

Results

Immunolocalization of Cftr in wild type mouse ameloblasts

Preliminary staining of wild type and knockout tissues with a commercially available monoclonal antibody (24-1) suggested that this antibody was not monospecific. Several other antibodies were then obtained which are often used in Cftr studies (review reference [35]) and their staining patterns in developing mouse teeth compared. Antibodies 3G11 and MD1314 produced virtually identical patterns of immunostaining, 24-1 differed in several aspects (Table 1).

In incisors of wild type mice 3G11 and MD1314 revealed a prominent positive staining in apical (facing enamel) plasma membrane of maturation ameloblasts (Fig. 2a, b, e) but not in presecretory or fully secretory ameloblasts (Fig. 2c). First (weak) staining was noted in the cytoplasm of late secretory and transitional ameloblasts. In young mice a weak intracellular staining was also seen in the adjacent stratum intermedium and stellate reticulum. MD1314 very occasionally gave a weak staining over the nuclei in a few secretory ameloblasts, odontoblasts and bone cells (not shown). Sections in which primary antibodies had been replaced by non-immune IgG were negative (not shown).

Staining with mouse 24-1 antibody showed a different pattern. The apical plasma membrane of maturation ameloblasts was immunopositive as well but less conspicuous than with the other two antibodies due to a consistent and robust cytoplasmic staining (Fig. 2f). A weak diffuse staining with 24-1 was already noted in secretory ameloblasts (Fig. 2d) in contrast to 3G11 (Fig. 2c) and MD1314 that were negative. Staining with 24-1 was also more widely distributed over other cells including non-epithelial cells (see below). This pattern did not change after several rounds of blocking of endogenous mouse IgG.

Staining of sagittal sections of lower incisors with 3G11 or MD1314 persisted in all maturation ameloblasts from early to late stages without overt interruption by non-stained cells (Fig. 3a). Only occasionally a small gap of some unstained maturation ameloblasts was seen with their apical end either damaged or not present in the plane of the section. In early maturation phase staining formed a broad fuzzy but intense band over the apical membrane and later became thinner and sharper in mid- and late-maturation cells.

Basically similar data as in incisors were found in mouse molar tooth germs: apical ends of maturation ameloblasts including ameloblasts on the enamel-free area at the tip of the cusps stained strongly with MD1314 and 3G11 (Fig 4a, b, d), whereas 24-1 gave a more widely distributed cytoplasmic staining (Fig. 4c).

Changes in ameloblast structure of incisors in Cftr-null mice

Cftr-null mice were viable but generally smaller than wild type littermates, and all their teeth erupted. Unlike wild type incisors that were orange-pigmented incisors of mutant mice were chalky white and showed substantial abrasion in agreement with previous reports [18,19]. Molar teeth of *Cftr* knockout mice did not show overt changes.

Structural changes were seen in maturation stage ameloblasts of adult *Cftr*-knockout mice, but presecretory and secretory cells looked normal, similar as reported [18]. Polarization of the maturation ameloblasts was gradually lost in mutant incisors, the cells shortened, and nuclei became round (Fig. 3b, 3c). The cells accumulated yellow-brown grains and later also fat-like droplets of various sizes not seen in wild type cells. All these changes were much more prominent in older adult mutant mice than in young mutant mice.

Validation of the specificity of the antibodies

In knockout tissues 3G11 and MD1314 failed to stain incisor maturation ameloblasts at normal antibody working dilutions that gave a strong staining in apical membrane (Fig. 3d–g). However, by increasing the concentration of primary antibodies 3 fold also MD1314 gave a weak cytoplasmic reaction in maturation ameloblasts in null mutants (not shown). Antibody 24-1 consistently showed a very strong cytoplasmic staining in null-mutant ameloblasts without a clear apical staining (Fig. 3h, 3i).

Immunostaining in mineralizing connective tissue cells

Surprisingly, some of the antibodies also stained mineralizing connective tissue cells (Fig. 4). Antibody 3G11 gave no in connective tissue cells including bone and pulp (Fig. 4a) but with 24-1 a fine granular intracellular staining was seen in odontoblasts, osteoblasts, osteocytes and some osteoclasts (Fig 4c, g; Table 1). This staining with 24-1 was moderate in developing mouse tissues but very strong in developing hamster jaws (Fig. 4c, g). Also human embryonic bone- and dentin-forming cells stained positive with 24-1 (not shown). With MD1314 staining in odontoblasts and bone cells of rodents was weak and variable (Fig. 4d).). In *Cftr*-null mice a strong (24-1) or variable but weak (MD1314) staining persisted in odontoblasts and bone cells.

A recent report showing 24-1 immunostaining of human bone cells [36] prompted us to investigate whether this staining was CFTR-specific. The human specific antibody CC-24 raised to a completely different portion of CFTR than 24-1 (Fig. 1) gave a similar granular cytoplasmic staining in odontoblasts (Fig. 4e) and bone cells of fetal human jaws, including preosteoblasts, osteoblasts, osteocytes and some of the osteoclasts (Fig. 4f, h, i). In control tissues CC24 stained luminal plasma membranes of rectum glands of healthy humans but failed to do so in biopsies from Δ F508 CF patients (not shown).

Transcipts for Cftr and CFTR

By RT-PCR transcripts for *Cftr* were detected in mouse osteoblast-like cells (MC3T3), human primary osteoblasts, rat maturation ameloblasts, and human dental pulp tissue including odontoblasts, but not in murine tongue (Fig. 5). Starting with an equal amount of RNA the positive controls (mouse kidney, human Universal reference mRNA) started to become visible after 30 cycles. The appearance of transcripts in cells from pulp and bone required at least 35 cycles indicating that expression in mineralizing connective tissue cells was much lower than in soft tissues with established *Cftr* expression. Sequencing of the amplified fragments confirmed that they originated from mouse *Cftr* and human *CFTR*-mRNA.

Discussion

Cftr and enamel formation

Our data are consistent with the hypothesis that Cftr channels are present in mouse ameloblasts and functionally active in pH regulation in incisors as previously suggested [18,19,20,22,23]. Here we demonstrate that Cftr immunostaining is not present in secretory ameloblasts but highly prominent in the apical plasma membranes of maturation ameloblasts, the cells that are severely affected in *Cftr*-null mutant mice ([18], present data). All maturation ameloblasts were immunostained for Cftr. This staining pattern is different from that for anion exchanger isoform 2 (Ae2), in which small groups of maturation ameloblasts - presumably smooth-ended cells - did not stain or stained only patches of their cell bodies [37,38]. The fact that after eruption incisor enamel rapidly erodes [18, present data) and contains less calcium than wild type incisors [19,29] demonstrates that *Cftr* is critical for functioning of maturation ameloblasts, similar as *Ae2* [37,38].

The molecular mechanisms responsible for buffering protons during amelogenesis are largely unknown. During secretory phase amelogenins are abundantly present in the enamel space and will likely buffer a major part of the protons [21,22]. However, when amelogenins have been removed in maturation stage, it is very conceivable that bicarbonates are secreted into the enamel space to buffer protons [21,24,]. Several reports speculated how ameloblasts could regulate pH changes in enamel by producing [39,40] and secreting bicarbonates using carbonic anhydrase and a set of (largely unknown) ion exchangers/cotransporters and chloride channels in the plasma membranes including Cftr [22–24]. In a recent model it was proposed that secretory ameloblasts import and secrete bicarbonates through activity of apical Ae2a and basolateral sodium bicarbonate cotransporter 1 (Nbc1) [41]. Previous [18,23] and present data strongly suggest that in maturation stage Cftr is a critical factor in pH regulation and essential for completion of enamel mineralization. In figure 6 we present a more detailed working model for the function of Cftr in (ruffle-ended) ameloblasts.

The model is principally based on pH regulation by cells of pancreatic duct that generate and secrete large quantities of bicarbonates into the lumen of the ducts [for review see 3,5,42]. The model builds on recent reports of enamel defects in knockout mice deficient in *Ae2* [38,39], *Nbc1* [43] and *Cftr* [18, present study]. In the model Cftr in ameloblasts has three major functions: (*i*) As classical chloride channel Cftr transduces intracellular Cl^- into the enamel space (Fig. 6). Anion-transporters in the apical plasma membranes that colocalize with Cftr exchange the extracellular Cl^- for intracellular bicarbonates. These anion-transporters are likely member(s) of the solute carrier family 26a (Slc26a) [5,44]. Slc26a is a group of 10 different members of multifunctional anion transporters, some of which exchange one Cl^- for one bicarbonate (electroneutral exchange, *e.g*., Slc26a4), while others exchange with different stoichiometry (electrogenic exchange, *e.g*, one Cl− for two bicarbonates as for Slc26a6 or two Cl^- for one bicarbonate as for Slc26a3;[44]). Electrogenic exchange influences membrane potential of the plasma membranes and thus the rate of efflux or influx of anions. (*ii*) Cftr also

controls bicarbonate efflux by directly stimulating the transport activity of Slca26 members and *vice versa*. Coexpression studies in cell lines showed that the Cftr molecule physically interacts through its R- (regulatory-) domain with the STAS-domain (Sulphate Transporter and Anti-Sigma factor antagonist) of Slc26a3 and Slc26a6 [44,45]. This interaction results in 5–6 fold enhanced transport activity by Slca26 [44,45]. (*iii*) Cftr on its own is also permeable for bicarbonate [2,4]. Though earlier studies showed that Cftr is 3–4 fold less permeable for bicarbonate than for Cl^- more recent studies in pancreatic duct cells show that Cftr can contribute up to 60% of the total amount of bicarbonate efflux [4].

In addition to cytosolic carbonic anhydrase type 2 maturation ameloblasts also express mRNA transcripts of carbonic anhydrase type 6 (*Car6*), a secreted type of carbonic anhydrase that may operate in maturation enamel, where it could catalyse the formation of CO_2 and H_2O from carbonic acid formed by bicarbonate buffering of the protons in the enamel space ([46], Fig. 6). However, the translation into protein and the localization of Car6 protein have not been assessed yet.

How pH is regulated in smooth-ended ameloblasts and how Cftr functions in this cell type is presently unknown. The substantial morphological changes that occur when ruffle-ended cells transform into smooth-ended cells including the temporary disappearance of lateral H^+K^+-ATPase activity [47] and possibly also Ae2 [37,38] suggest that smooth-ended cells function fundamentally different from ruffle-ended cells.

Collectively, these data confirm previous reports that *Cftr* is critical for enamel mineralization in mouse incisors. Cftr potentially functions as regulator of pH in the enamel fluid by conducing Cl^- and bicarbonates into enamel and by stimulating the activity of several (hypothetic) types of anion transporters to secrete bicarbonates.

Antibody specificity and cftr in bone cells

A striking finding was that also bone cells express Cftr. Using antibody 24-1 Shead et al. [36] reported cytoplasmic immunostaining in normal human fetal bone cells and showed the presence of the expected mature (fully glycosylated) 180 kD protein in bone tissue extracts. However, considering the well-established apical localization of human CFTR in T84 cells [48], used as a positive control in the Shead study, it is remarkable that their immunostaining of T84 cells with 24-1 was cytoplasmic, with strong perinuclear staining [36]. We report here that antibody 24-1 does not react exclusively with Cftr but also detects epitopes different from Cftr; this was demonstrated by a very strong immunostaining of maturation ameloblasts in *Cftr*-deficient ameloblasts. In support of this it is also pertinent to report that by Western blotting with 24-1 but not with 3G11 and MD1314 we can detect immunopositive bands in extracts from intestine of *Cftr*-null mice showing a similar molecular weight as authentic Cftr (de Jonge et al. unpublished data). This also indicates that 24-1 is not monospecifc and thus the positive staining in bone cells [36] may not merely reflect the presence of Cftr protein. In a more extensive study we here present evidence that mouse and human bone cells contain low levels of *Cftr* mRNA and are positively stained by at least two monospecific antibody species in addition to 24-1. These findings strongly support the concept that osteoblasts and odontoblast do express low amounts of Cftr protein.

Both CF patients and *Cftr*-deficient mice are known to develop osteopenia [49–52], even in the absence of overt respiratory and gastrointestinal diseases or steroid treatment [50,51]. Three weeks old *Cftr*-deficient mice had reduced bone mineral density and increased bone resorption relative to bone formation [50]. In skeletally mature (28-weeks old) mutant mice some of these bone defects had improved compared with 12-weeks old mutants but defects persisted in cortical and trabecular bone structure [51]. Based on the increase in the number of osteoblasts and osteoclasts it was suggested that peak bone mass in *Cftr*-deficient mice may have been

delayed and bone turnover increased compared with age-matched wild type mice [51]. Our data show that Cftr protein is present in murine and human bone cells. Expression of Cftr in bone cells and odontoblasts was not seen in plasma membranes but intracellular. There is evidence that *Cftr* is expressed at a low level in membranes of organelles in other non-epithelial cell types, *e.g.* lymphocytes, phagocytes, alveolar macrophages and muscle tissue [53–59]. In some of these cell types Cftr has been implied to act as Cl^- channel for phagosomal acidification in alveolar macrophages [55,56], but other studies question such a function [57,58]. Skeletal muscle has been shown to express low levels of Cftr in the sarcoplasmic reticulum, and calcium homeostasis was dysregulated in *Cftr*-deficient muscles [59]. In analogy with these cell types Cftr in bone cells may likewise function as a Cl^- channel or glutathione transporter [59] in intracellular organelles. Poor functioning of Cftr in organelle membranes of bone cells may underlie the changes in bone metabolism in *Cftr*-deficient mice or in CF patients, resulting in osteopenia.

In conclusion, we report here that maturation ameloblasts in rodents express Cftr in their apical plasma membrane. The data suggest that Cftr may functionally be involved in pH regulation. Bone- and dentin-forming cells express Cftr mainly intracellularly but the function of Cftr in this compartment remains to be elucidated. Poor functioning of Cftr in *Cftr*-deficient bone cells may be responsible for development of osteopenia.

Acknowledgments

The authors acknowledge Dr.V. Everts for his helpful comments.

This work was supported by NIH grant DE13508-06 (DL, THB, PdB and AB)

References

1. Collins FS. Cystic fibrosis: a molecular biology and therapeutic implications. Science 1992;256:774–779. [PubMed: 1375392]
2. Shcheynikov N, Kim KH, Kim K, Dorwart M, Ko SBH, Goto H, Naruse S, Thomas PJ, Muallem S. Dynamic control of cystic fibrosis transmembrane conductance regulator Cl^-/HCO_3^- selectivity by external Cl^-. J Biol Chem 204(279):21857–21865.
3. Ishiguro H, Steward M, Naruse S. Cystic fibrosis transmembrane conductance regulator and Slc26 transporters in HCO3 secretion by pancreatic duct cells. Acta Physiol Sinica 2007;59:465–476. [PubMed: 17700966]
4. Ishiguro H, Steward MC, Naruse S, Ko SB, Goto H, Case RM, Kondo T, Yamamoto A. CFTR functions as a bicarbonate channel in pancreatic duct cells. J Gen Physiol 2009;33:315–326. [PubMed: 19204187]
5. Steward MC, Ishiguro H, Case RM. Mechanisms of bicarbonate secretion in the pancreatic duct. Ann Rev Physiol 2005;67:377–409. [PubMed: 15709963]
6. Lindsell P. Mechanism of chloride permeation in the cystic fibrosis transmembrane conductance regulator chloride channel. Exp Physiol 2006;91:123–129. [PubMed: 16157656]
7. Trezise A, Buchwald M. In vivo cell-specific expression of the cystic fibrosis transmembrane conductance regulator. Nature 1991;353:434–437. [PubMed: 1716739]
8. Tizzano E, Chitayat D, Buchwald M. Cell-specific localization of CFTR mRNA shows developmentally regulated expression in human fetal tissues. Hum Mol Gen 1993;2:219–224. [PubMed: 7684640]
9. Webster P, Vanacore L, Nairn A, Mariono C. Subcellular localization of CFTR to endosomes in a ductal epithelium. Am J Physiol 1994;267:C340–C348. [PubMed: 7521124]
10. Zeng W, Lee MG, Yan M, Diaz J, Benjamin I, Marino CR, Kopito R, Freedman S, Cotton C, Muallem S, Thomas P. Immuno and functional characterization of CFTR in submandibular and pancreatic acinar and duct cells. Am J Physiol 1997;273:C442–C455. [PubMed: 9277342]

11. Ameen N, Alexis J, Salas P. Cellular localization of the cystic fibrosis transmembrane conductance regulator in mouse intestinal tract. Histochem Cell Biol 2000;114:69–75. [PubMed: 10959824]
12. Claass A, Sommer M, de Jonge H, Kälin N, Tümmler B. Applicability of different antibodies for immunohistochemical localization of CFTR in sweat glands from healthy controls and from patients with cystic fibrosis. J Histochem Cytochem 2000;48:831–838. [PubMed: 10820156]
13. Wioland MA, Fleury-Feith J, Corlieu P, Commo F, Monceaux G, Laucau-St-Guily J, Bernaudin JF. CFTR, MDR1 and MDRP1 immunolocalization in normal human nasal respiratory mucosa. J Histochem Cytochem 2000;48:1215–1222. [PubMed: 10950878]
14. Zegarelli EV, Kutscher AH, Denning CR, Applebaum E, Fahn BS, Hoffman PJ, Botwick JT, Ragosta JM. Discoloration of the teeth in older children with cystic fibrosis of the pancreas. Am J Dig Dis 1964;9:682–683. [PubMed: 14215820]
15. Primosch RE. Tetracycline discoloration, enamel defects, and dental caries in patients with cystic fibrosis. Oral Surg, Oral Med, Oral Path 1989;50:301–308. [PubMed: 6935580]
16. Azevedo TD, Feijo GS, Bezerra AC. Presence of developmental defects of enamel in cystic fibrosis patients. J Dent Child 2006;73:159–163.
17. Cua FT. Calcium and phosphorus in teeth from children with and without cystic fibrosis. Biol Trace Elem Res 1991;30:277–289. [PubMed: 1720648]
18. Wright JT, Kiefer CL, Hall KI, Grubb BR. Abnormal enamel development in a cystic fibrosis transgenic mouse model. J Dent Res 1996;75:966–973. [PubMed: 8708137]
19. Wright JT, Hall KI, Grubb BR. Enamel mineral composition of normal and cystic fibrosis transgenic mice. Adv Dent Res 1996;10:270–275. [PubMed: 9206347]
20. Arquitt CK, Boyd C, Wright JT. Cystic Fibrosis Transmembrane Regulator Gene (CFTR) is associated with abnormal enamel formation. J Dent Res 2002;81:492–496. [PubMed: 12161463]
21. Simmer JP, Fincham AG. Molecular mechanisms of dental enamel formation. Crit Rev Oral Biol Med 1995;6:84–108. [PubMed: 7548623]
22. Smith CE. Cellular and chemical events during enamel maturation. Crit Rev Oral Biol Med 1998;9:128–161. [PubMed: 9603233]
23. Sui W, Boyd C, Wright JT. Altered pH regulation during enamel development in the cystic fibrosis mouse incisor. J Dent Res 2003;82:388–392. [PubMed: 12709507]
24. Smith CE, Chong DL, Bartlett JD, Margolis HC. Mineral acquisition rates in developing enamel on maxillary and mandibular incisors of rats and mice: implications to extracellular acid loading as apatite crystals mature. J Bone Miner Res 2005;20:240–249. [PubMed: 15647818]
25. Josephsen K, Fejerskov O. Ameloblast modulation in the maturation zone of the rat incisor enamel organ. A light and electronmicrocopic study. J Anat 1977;124:45–70. [PubMed: 914705]
26. Smith CE, McKee M, Nanci A. Cyclic induction and rapid movement of sequential waves of new smooth-ended ameloblast modulation bands as visualized by polychrome fluorescent labeling and ghba staining of maturing enamel. Adv Dent Res 1987;1:162–175. [PubMed: 2461208]
27. Sasaki S, Takagi T, Suzuki M. Cyclic changes in pH in bovine developing enamel as sequential bands. Arch Oral Biol 1991;36:227–231. [PubMed: 1877895]
28. Smith CE, Issud, Margolis HC, Moreno EC. Developmental changes in the pH of enamel fluid and its effects on matrix resident proteinases. Adv Dent Res 1996;10:159–169. [PubMed: 9206332]
29. Gawenis LR, Spencer P, Hillman LS, Harline MC, Morris JS, Clark LL. Mineral content of calcified tissues in cystic fibrosis mice. Biol Trace Elem Res 2001;83:69–81. [PubMed: 11694004]
30. Ratcliff R, Evans MJ, Cuthbert AW, MacVinish LJ, Foster D, Anderson JR, Colledge WH. Production of a severe cystic fibrosis mutation by gene targeting. Nature Gen 1993;4:35–41.
31. French PJ, Doorninck JH, Peters RHPC, Verbeek E, Ameen NA, Marino CR, De Jonge HR, Bijman J, Scholte BJ. A DF508 mutation in mouse cystic fibrosis transmembrane conductance regulator results in a temperature-sensitive processing defect in vivo. J Clin Invest 1996;98:1304–1312. [PubMed: 8823295]
32. Broere N, Hillesheim J, Tuo B, Jorna H, Houtsmuller AB, Shenolikar S, Weinman EJ, Donowitz M, Seidler U, De Jonge HR, Hogema BM. Cftr is reduced in the small intestine of Na+/H+ exchanger 3 regulatory factor 1 (NHERF-1) but not of NHERF-2 deficient mice. J Biol Chem 2007;282:37575–37584. [PubMed: 17947234]

33. Lewis HA, Buchanan SG, Burley SK, Conners K, Dickey M, Dorwart M, Fowler R, Gao X, Guggino WB, Hendrickson WA, Hunt JF, Kearins MC, Lorimer D, Maloney PC, Post KW, Rajashankar KR, Rutter ME, Sauder JM, Shriver S, Thibodeau PH, Thomas PJ, Zhang M, Zhao X, Emtage S. Structure of nucleotide-binding domain 1 of the cystic fibrosis transmembrane conductance regulator. EMBO J 2004;23:282–293. [PubMed: 14685259]
34. Picciotto MR, Cohn JA, Bertuzzi G, Greengard P, Nairn AC. Phosphorylation of the cystic fibrosis transmembrane conductance regulator. J Biol Chem 1992;267:12742–52. [PubMed: 1377674]
35. Mendes F, Farinha CM, Roxo-Rosa M, Fanne P, Edelman A, Dormer R, McPhersn M, Davidson H, Puchelle E, De Jonge H, Heda GD, Gentzsch M, Lukacs GL, Penque D, Amaral MD. Antibodies for CFTR studies. J Cystic Fibrosis 2004;3:69–72.
36. Shead E, Haworth C, Condliffle A, McKeon D, Scott M, Comston J. Cystic fibrosis transmembrane conductance regulator (CFTR) is expressed in human bone. Thorax 2007;62:650–651. [PubMed: 17600296]
37. Lyaruu DM, Bronckers AL, Mulder L, Mardones P, Medina JF, Kellokumpu S, Oude Elferink RP, Everts V. The anion exchanger Ae2 is required for enamel maturation in mouse teeth. Matrix Biol 2008;27:119–127. [PubMed: 18042363]
38. Bronckers ALJJ, Lyaruu DM, Jansen DC, Medina JF, Kellokumpu S, Hoeben KA, Gawennis LR, Oude Elferink RPJ, Everts V. Localization and function of the anion exchanger Ae2 in developing teeth and orofacial bones in rodents. J Exp Zool 2009;312B:375–387.
39. Sugimoto T, Ogawa Y, Kuwahara H, Shimazaki M, Yagi T, Sakai A. Histochemical demonstration of carbonic anhydrase activity in the odontogenic cells of the rat incisor. J Dent Res 1988;67:1271–1274. [PubMed: 3139725]
40. Toyosawa S, Ogawa Y, Inagaki T, Ijuhin N. Immunohistochemical localization of carbonic anhydrase isozyme II in rat incisor epithelial cells at various stages of amelogenesis. Cell Tissue Res 1996;285:217–225. [PubMed: 8766158]
41. Paine ML, Snead ML, Wang HJ, Abuladze N, Pushkin A, Liu W, Kao LY, Wall SM, Kim YH, Kurtz I. Role of NBCe1 and AE2 in secretory ameloblasts. J Dent Res 2008;87:391–195. [PubMed: 18362326]
42. Soleimani M, Burnham CE. Na+: HCO3− cotransporters (NBC). Cloning and characterization. J Membr Biol 2001;183:71–84. [PubMed: 11562789]
43. Gawenis LR, Bradford EM, Prasad V, Lorenz JN, Simpson JN, Simpson JE, Clark LL, Woo AL, Grisham C, Sandford LP, Doetschman T, Miller ML, Shull GE. Colonic anion secretrory defects and metabolic acidosis in mice lacking the NBC1 Na+/HCO3− cotransporter. J Biol Chem 2007;282:9042–52. [PubMed: 17192275]
44. Mount DB, Romero MF. The SLC26 gene family of multifunctional anion exchangers. Pflugers Arch Eur J Physiol 2004;447:710–721. [PubMed: 12759755]
45. Ko SB, Zeng W, Dorwart MR, Luo X, Kim KH, Millen L, Goto H, Naruse S, Soyombo A, Muallem TPJ. Gating of CFTR by the STAS domain of SLC26 transporters. Nat Cell Biol 2004;6:292–294. [PubMed: 15057243]
46. Smit CE, Nanci A, Moffat P. Evidence by signal peptide trap technology for the expression of carbonic anhydrase 6 in rat incisor enamel organs. Eur J Oral Sci 2006;114(S1):147–153.
47. Sasaki T, Tadokoro K, Yanagisawa S, Garant PR. H+-K+-ATPase activity in the rat incisor enamel organ during enamel formation. Anat Rec 1988;221:823–33. [PubMed: 2847591]
48. Denning GM, Ostedgaard LS, Cheng SH, Smith AE, Welsh MJ. Localization of cystic fibrosis transmembrane conductance regulator in chloride secretory epithelia. J Clin Invest 1992;89:339–349. [PubMed: 1370301]
49. Boyle MP. Update on maintaining bone health in cystic fibrosis. Curr Opin Pulm Med 2006;12:453–458. [PubMed: 17053497]
50. Dif F, Marty C, Baudiun C, de Vernejoul MC, Levi G. Severe osteopenia in CFTR-null mice. Bone 2004;35:595–603. [PubMed: 15336594]
51. Haston CK, Li W, Li A, Lafleur M, Henderson JE. Persistent osteopenia in adult cystic fibrosis transmembrane conductance regulator-deficient mice. Am J Resp Crit Care Med 2008;177:309–315. [PubMed: 18006890]

52. Aris RM, Guise TA. Cystic fibrosis and bone disease: are we missing a genetic link? Eur Resp J 2005;25:9–11.

53. Bubien J. CFTR plays a role in regulated secretion by lymphocyte: a new hypothesis for the pathophysiology of cystic fibrosis. Eur J Physiol 2001;443:36–39.

54. Painter RG, Valentine VG, Lanson NA Jr, Leidal K, Zhang Q, Lombard G, Thompson C, Viswanathan A, Nauseef WM, Wang G. CFTR expression in human neutrophils and the phagolysosomal chlorination defect in cystic fibrosis. Biochemistry 2006;45:10260–10269. [PubMed: 16922501]

55. Di A, Brown ME, Deriy LV, Li C, Szeto FL, Chen Y, Huang P, Tong J, Naren AP, Bindokas V, Palfrey HC, Nelson DJ. CFTR regulates phagosome acidification in macrophages and alters bactericidal activity. Nature Cell Biol 2006;8:933–944. [PubMed: 16921366]

56. Deriy LV, Gomez EA, Zhang G, Beacham DW, Hopson JA, Gallan AJ, Shevchenko PD, Bindokas VP, Nelson DJ. Disease causing mutations in the cystic fibrosis transmembrane conductance regulator determine the functional responses of alveolar macrophages. J Biol Chem. 2009 Oct 16; Epub ahead of print.

57. Haggie PM, Verkman AS. Cystic fibrosis transmembrane conductance regulator-independent phagosomal acidification in macrophages. J Biol Chem 2007;282:31422–31428. [PubMed: 17724021]

58. Barriere H, Bagdany M, Bossard F, Okiyoneda T, Wojewodka G, Gruenert D, Radzioch D, Lukacs GL. Revisiting the role of cystic fibrosis transmembrane conductance regulator and counterion permeability in the pH regulation of endocytic organelles. Mol Biol Cell 2009;20:3125–41. [PubMed: 19420138]

59. Divangahi M, Balghi H, Daniakou G, Comtois AS, Demoule A, Ernest S, Haston C, Robert R, Hanrahan JW, Radzioch D, Petrof BJ. Lack of CFTR in skeletal muscle predisposes to muscle wasting and diaphragm muscle pump failure in cystic fibrosis mice. PLoS Genet 2009 July 5;(7):e1000586. [PubMed: 19649303]

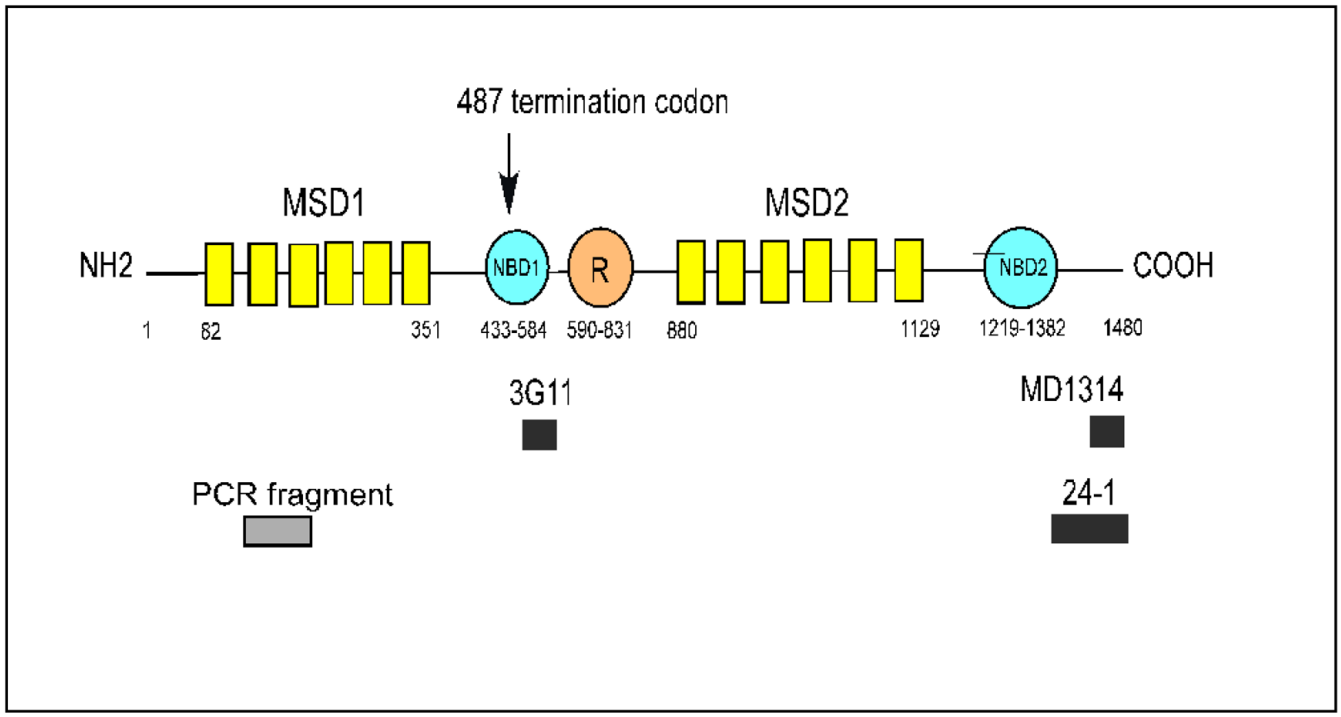

Fig 1. Schematic map of the domains in the human *CFTR* gene

MSD1 membrane spanning domain 1; NBD1 nucleotide binding domain 1; R regulatory domain; MSD2 membrane spanning domain 2; NBD2 nucleotide binding domain 2. The figures below the domains indicate amino acid numbering from 1-1480 of the hCFTR protein. To generate the *Cftr* knockout mouse strain a stop codon was inserted in the mouse gene after amino acid 487. The small black bars below the domains indicate approximate positions of the peptide sequences in human CFTR (or of corresponding sequences in mouse Cftr) used to generate antibody 3G11, CC24, MD1314 and 24-1. The grey bar indicates the position of the fragments for which the nucleotide sequence was detected by RT-PCR (Drawn and modified after: http://www.genet.sickkids.on.ca/cftr)

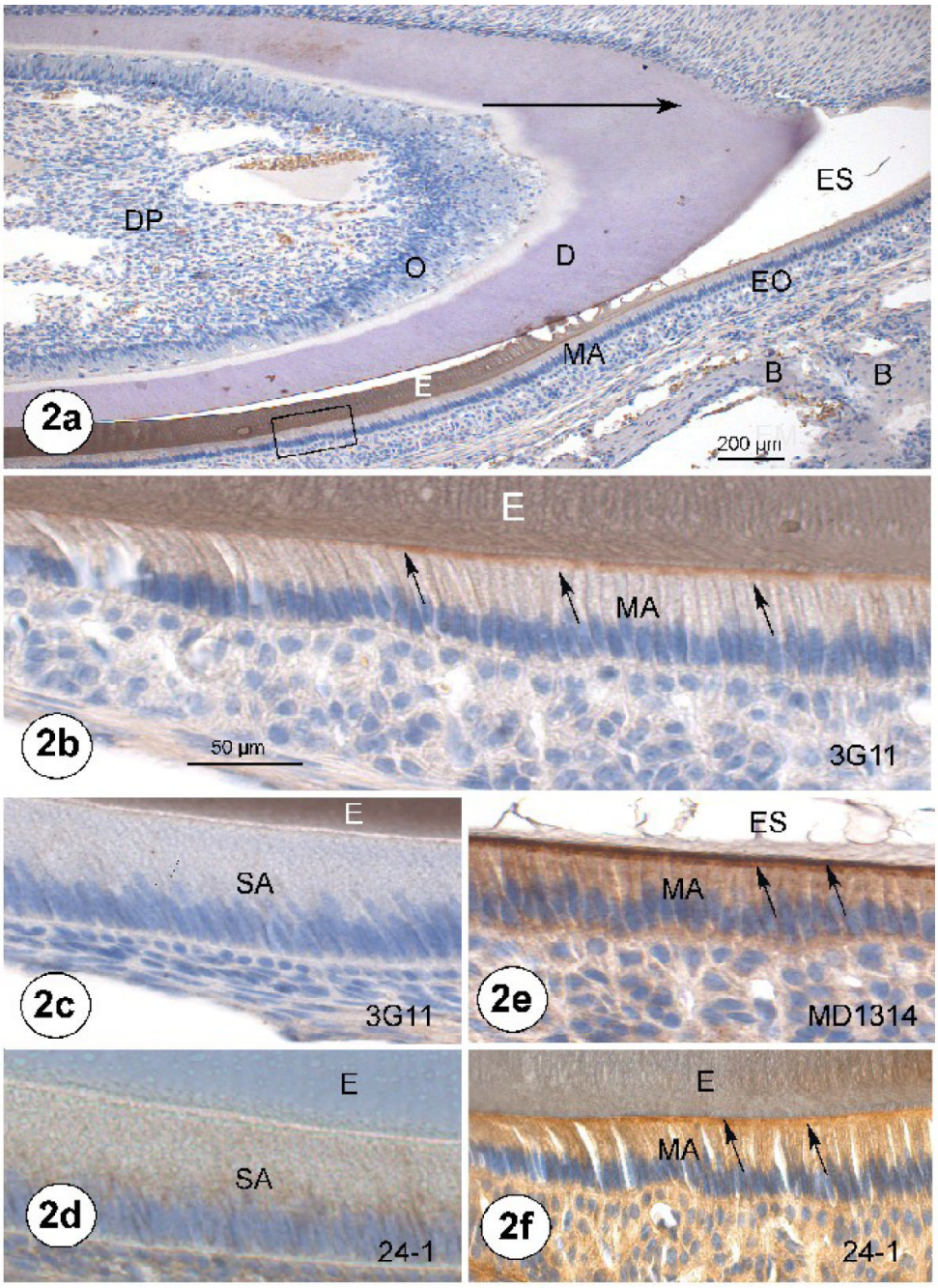

Fig. 2. Developmental expression and location of Cftr-protein in young mandibular mouse incisors using different antibodies

(a) Incisal part of incisor stained with antibody 3G11. At the bottom left of boxed area: late secretory stage ameloblasts deposit the last matrix into the enamel space on top of dentin (D). To the right of the boxed area they are maturation ameloblasts (MA) ameloblasts. B bone; DP dental pulp; E enamel; EO enamel organ; ES enamel space. The boxed area is enlarged in Fig. 2b.

(b) Magnification of boxed area of Fig 2a. Arrows indicate a brown-orange positive staining at the apical end of young maturation ameloblasts facing the enamel (E). Faint staining in cytoplasm. Staining with 3G11

(c) Secretory ameloblasts (SA) along forming enamel (E) do not stain with 3G11
(d) Secretory ameloblasts (SA) stain diffusely with 24-1
(e) Maturation stage ameloblasts (MA) stain with MD1314. Arrows indicate a very strong positive staining over apical membrane. ES enamel space
(f) Maturation stage ameloblasts (MA) stain substantially, arrows point to positive staining over apical membrane not as conspicuous as in Fig 2e.
Adjacent sections from the same tissue block were used. Large arrow in Fig. 2a points into incisal direction; also for Figs 2b–f. Counterstaining hematoxylin. Original magnifications: a. 250× ; b-f 400×. Calibration bars indicate length in μm.

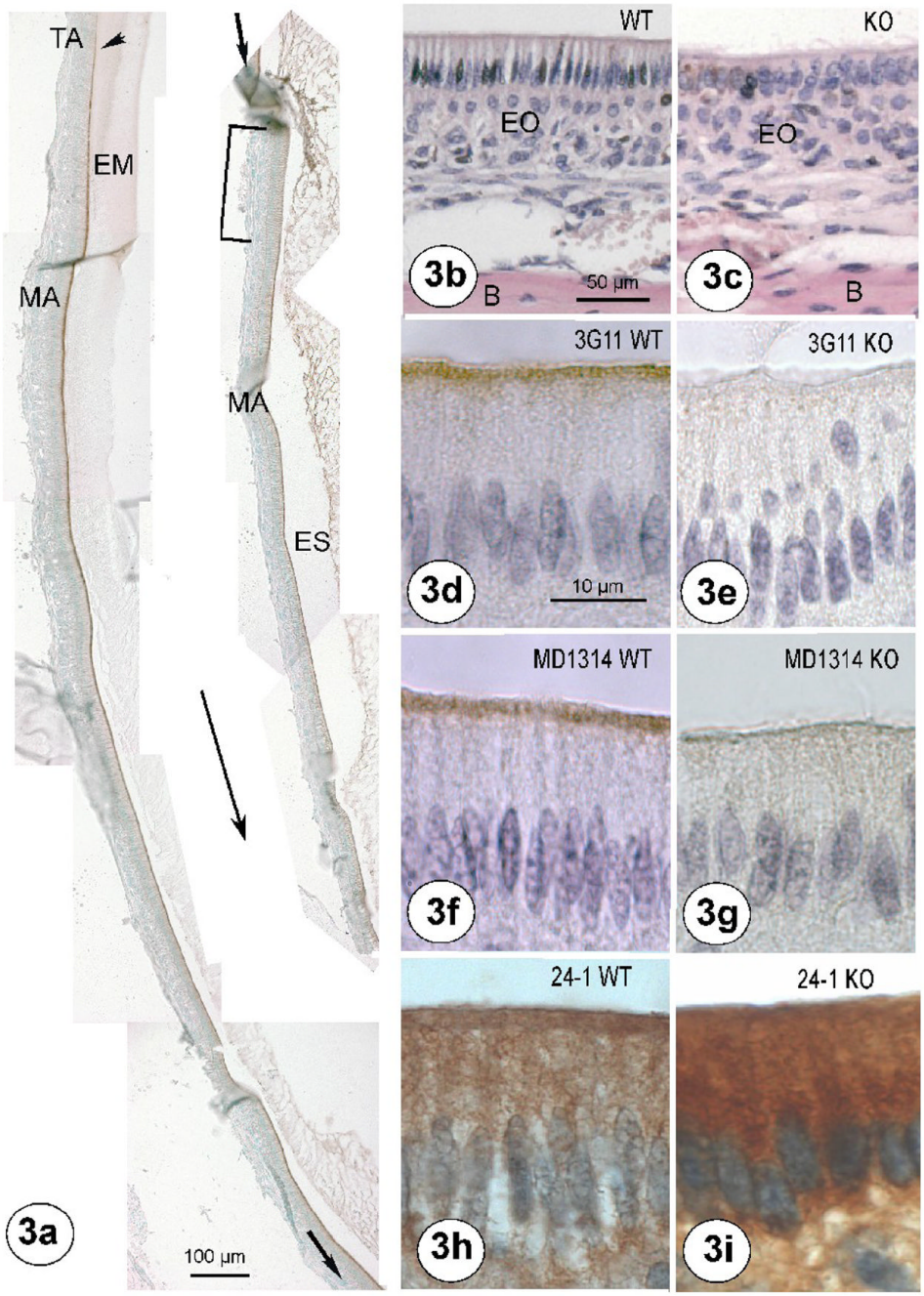

Fig. 3. Low power view of immunostaining in maturation stage of an adult wild type mouse incisor (a), structural changes in knockout ameloblasts (b, c) and validation of antibodies tested on sections of *Cftr*-null mutants (d–i)

(a.) Two consecutive parts of a lower incisor of an adult wild type mouse sectioned sagittally and stained with MD1314. At the top left the first immunostaining becomes apparent (arrowhead) near transitional ameloblasts (TA). More incisally (in the direction of the large arrow) maturation ameloblasts (MA) stain strongly over their apical membranes. The bottom end of the incisor part (small arrow) continues with the second part of the incisor at the top right (small arrow). Staining at the apical end of the ameloblasts is uninterrupted except for a

small group of cells (bracket) that did not include their apical part in the plane of sectioning. The most incisal part of the incisor was lost during the histological procedures.
(b, c) Early maturation ameloblasts of an incisor of a wild type (WT) and knockout (KO) adult mouse. EO enamel organ. B bone (HE staining)
(d, e) Wild type and knockout maturation ameloblasts stained with 3G11.
(f, g) Wild type and knockout maturation ameloblasts stained with MD1314.
(h, i) Wild type and knockout maturation ameloblasts stained with 24-1.
Counterstaining hematoxylin. Original magnifications: a. 100×; b, c, 400×; d-i; 1000×. Calibration bars indicate length in μm.

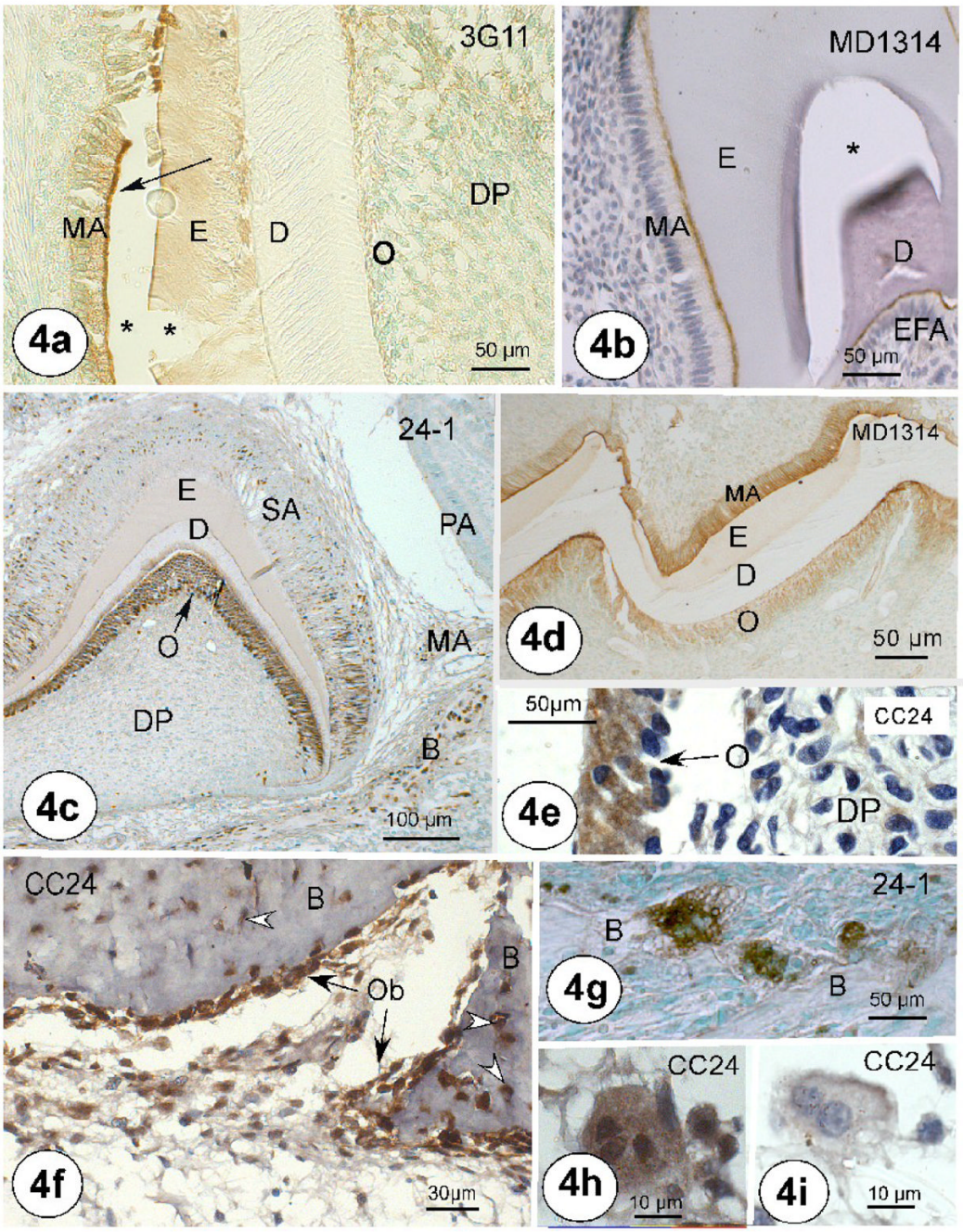

Fig. 4. Immunostaining for Cftr in developing molar tooth germs and bones

(a) Wild type mouse molar tooth germ stained with 3G11. Apical membranes of maturation ameloblasts (MA) are immunopositive, odontoblasts (O) and cells of dental pulp (DP) are immunonegative. Undecalcified section, * preparation artefacts

(b) Wild type mouse molar tooth germ stained with MD1314. Strong staining is present in maturation ameloblasts (MA). Bottom right: staining in ameloblasts along enamel free area (EFA). D dentin, E enamel, Decalcified, * shrink artefact

(c) Hamster first molar tooth germ stained with 24-1. Secretory ameloblasts (SA) are positive with discrete intracellular staining, also seen in other cells of the enamel organ. Very prominent distinct cytoplasmic staining is seen in odontoblast layer (O) and in bone cells (B).

Preameloblasts (PA) of second molar tooth germ are immunonegative. DP dental papilla, E enamel D dentin

(d) Mouse molar tooth germ stained with 3-fold normal working concentration MD1314. Maturation ameloblasts (MA) show strong apical staining and varying staining in cytoplasm. Note a weak staining in the odontoblasts (O) layer. ES enamel space, D dentin. The staining in odontoblast (O) layer varies from very weak to moderate positive.

(e) Odontoblasts (o) of a human fetal incisor stained with human specific CC24.

(f) Developing alveolar bone of human fetal jaw stained with CC24.

(g) Positive osteoclasts in hamster alveolar bone stained with 24-1

(h, i)Positive and negative human osteoclasts from human alveolar bone stained with CC24 and counterstained with hematoxylin (b, e, f, h i, blue nuclei) and methyl green (a, c, d, green nuclei only weakly).

Original magnifications a, b, c 250×; c, d 100×; g 400×; inset f, e, h, i 1000× Calibration bars indicate length in μm

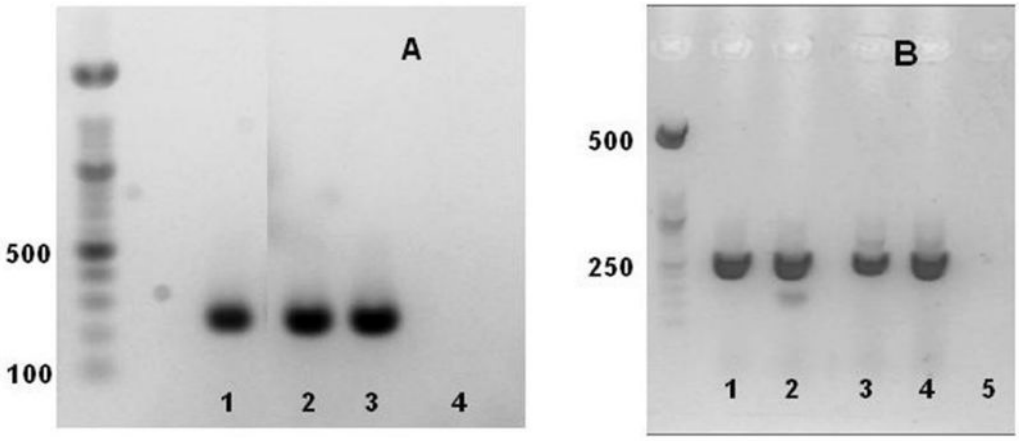

Fig. 5. Transcripts of *Cftr* in bone and dental cells of mouse/rat (A) and humans (B)

A: Lane 1: mouse MC3T3 osteoblast-like cells; lane 2: mouse kidney (positive control); lane 3: rat maturation stage ameloblasts; lane 4: mouse tongue (negative control). Mouse primers for exon 4-5, expected size 235 bp. Y-axis: nucleotide size (100 bp ladder)

B: lane 1: commercial human reference (positive control); lane 2: human dental pulp; lane 3: human osteoblasts (subject 1); lane 4: human osteoblasts (subject 2); lane 5: water (negative control). Human primers for exon 4-6, expected size 257 bp. Y-axis: nucleotide size (50 b)

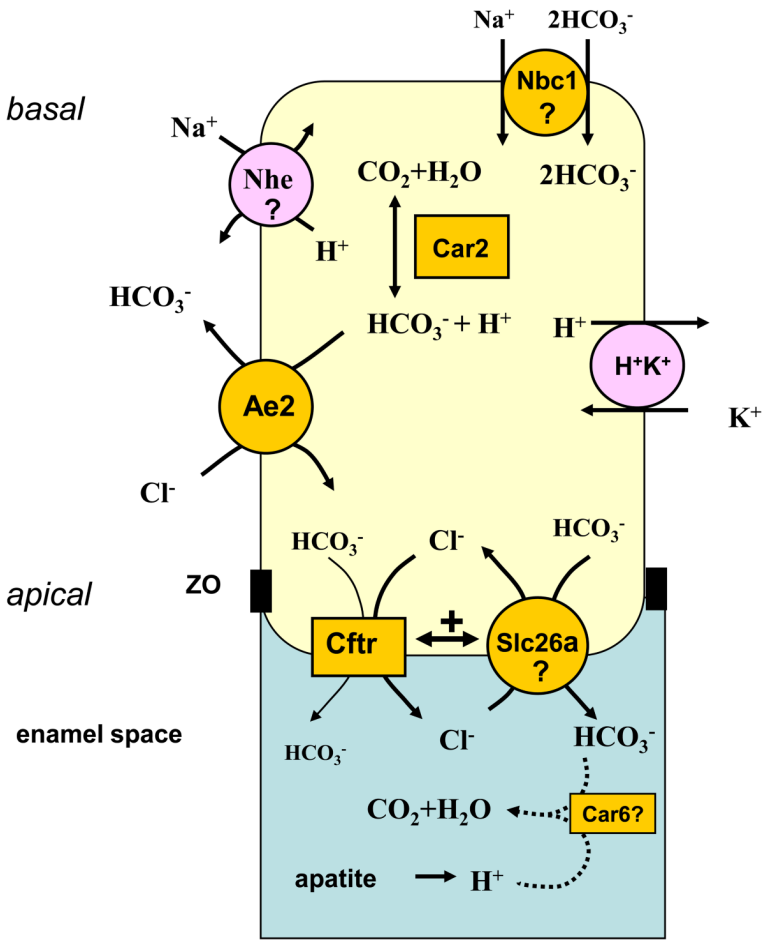

Fig 6. Working model depicting the putative role of Cftr in extracellular pH regulation by ruffle-ended ameloblasts

Apatite forms in the enamel space from ionic calcium, phosphate and water; this generates 8 protons per unit of cell hydroxyapatite [21]. These protons are buffered by bicarbonates secreted into the enamel space by maturation ameloblasts [21,23]. Bicarbonate is generated by activity of cytosolic carbonic anhydrase-type 2 (Car2, [39,40]). Bicarbonates are also imported through the basal plasma membrane plausibly by Na^+-$2HCO_3^-$ cotransporter isotype 1 (Nbc1 or Slc4a4, [42,43]). Intracellular bicarbonate is exchanged for Cl^- basolaterally by sodium-independent anion exchanger-2 (Ae2 or Slc4a2 [37,38]). At the apical plasma membrane the imported Cl^- is conduced into the enamel space through the Cftr channel ([23], present study). The extracellular Cl^- is then exchanged for one or more bicarbonates by (a) hypothetic member (s) of the anion transporter Slc26a family that colocalize(s) with Cftr [4,44]. Several Slc26a members may be present in the same apical membrane simultaneously. Cftr interacts physically with Slc26a members, which strongly stimulates (+) the exchange activity of the Slc26a [44, 45]. The Cftr can also be permeable for bicarbonates [2,4]. The electrogenic Nbc1 cotransporter at the basal membrane induces plasma membrane hyperpolarization; such sustained hyperpolarization stimulates HCO_3^- – efflux across the apical membrane. The bicarbonates secreted into the enamel space react with protons to form carbonic acid that can form CO_2 and water, catalyzed by a putative carbonic anhydrase 6 (Car6, [46]). Water is used partly to form new apatites, partly reabsorbed by ameloblasts. The CO_2 can pass the apical membrane and be reused intracellularly to form bicarbonate by Car2. To prevent intracellular acidification the protons generated by Car2 are pumped out by basolateral H^+/K^+ ATPase activity (H^+/K^+,

[47]) or by (a) hypothetic sodium hydrogen exchanger(s) (NEH, [5]). Any excess of intracellular sodium is exchanged for potassium by a Na^+/K^+-ATPase (not drawn). Question marks: hypothetic; ZO: zonula occludens

Table 1

Cftr staining in mouse incisors and bone

	24-1		MD1314		3G11	
Cell Type	**WT**	**KO**	**WT**	**KO**	**WT**	**KO**
Secretory ameloblasts	+/− to +	+/−	(+/−)	−	−	−
Transitional ameloblast	+/−	+/−	+/−	−	+/−	−
Maturation ameloblasts*	+++	+++	+++	(+/−)−(+)	+++	−
Stellate reticulum/papillary cells	++	++	+	−	+	−
Odontoblasts	+	+	(+/−)	+/−	+/−	−
Osteoblasts	+	+	(+/−)	−	+/−	−
Osteocytes	+	+	+/−	−	+/−	−
Osteoclasts	+	+	+/−	−	+/−	−

− negative, +/− weak, variable, + moderate, ++ strong, +++ very strong

*apical plasma membrane, WT= Cftr wild type mice; KO= Cftr knock out mice